1er SIMPOSIO INTERNACIONAL SOBRE SENSORES REMOTOS Y SISTEMAS DE INFORMACION GEOGRAFICA (SIG) PARA EL ESTUDIO DE RIESGOS NATURALES

INUNDACION DEL RIO ARAUCA

PASTO Y EL VOLCAN GALERAS

A DE IBAGUE

MEMORIAS

MEDIUM SCALE LANDSLIDE HAZARD ANALYSIS USING A PC-BASED GIS. A CASE STUDY FROM CHINCHINA, COLOMBIA

By
C.J. van Westen (*)

Abstract
Landslide hazard analysis techniques using a PC-based Geographical Information System were tested out in a mountainous area in the Central Cordillera in Colombia. Much emphasis was put on photo-interpretation of landslides, using photo-checklists, as well as using field checklists. From a large set of parameter maps, the relations between the various parameter classes and different landslide types were investigated via map crossing. Weight values were calculated by comparing the results with the overall density of the phenomena over the whole area. From the tables, containing the weight values, the most significant were selected and combined in landslide susceptibility maps.

Resumen
Algunos metodos para el analisis de amaneza por deslizamientos fueron aplicados en un area montanosa en la Cordillera Central de Colombia. Mucho enfasis fue dado a la fotointerpretacion de deslizamientos, utilizando listas de verificacion, tambien en el campo. A partir de un conjunto grande de mapas de parametros, las relaciones entre las diferentes clases de parametros y la occurencia de diferentes tipos de deslizamientos fueron investigadas, mediante el cruce de mapas. Valores de peso fueron calculados comparando los resultados con la densidad general del fenomeno, sobre todo el area. Desde las tablas con los valores de peso, los parametros mas significativos fueron seleccionados y combinados en un mapa de susceptibilidad para deslizamientos.

Introduction

In this papaer some of the preliminary results are presented of an extensive ongoing research on the applicability of Geographical Information Systems (GIS) for mountain hazard mapping. The investigation is carried out by a multidisciplinary group from various institutes in the Netherlands (ITC, Universities of Amsterdam and Utrecht), France (BRGM) and Colombia (IGAC, Universities in Manizales). The project is sponsored by UNESCO, the Dutch ministery of Education & Research and EC (See also Rengers, this volume).
Attention is given to the difference of objectives, input data and analysis techniques on various scales (Van Westen, this volume). Here some examples of analysis techniques on the medium scale, 1:25.000, will be presented.

(*) International Institute for Aerospace Survey and Earth Sciences ITC, PO box 6, 7500 AA Enschede, The Netherlands.

Results of other scales can be found in Rengers et al (1991, this volume), Soeters et al (1991), Van Westen (1989, 1990), Van Westen & Alzate (1991) and Van Asch et al (this volume).
The project narrows down the use of GIS to those systems which are based on relatively less expensive configurations using Personal Computers. The reason for this is that the analysis techniques for landslide hazard assessment should be applicable in regional offices of geological services, or other institutions responsible for this work, and therefore should be at low cost. In the framework of the project a representative PC-based GIS was chosen, called ILWIS (Integrated Land and Watershed Information System). This package, developed at ITC has all the standard tools available for image, map and attribute data handling (Valenzuela 1988).

The study area
The pilot study area for the project is located in the department of Caldas, Colombia, within the municipalities of Manizales, Villamaria, Palestina and Chinchina (see figure 1). The overall study area on the regional scale consists of the catchment of the Chinchina river and covers an area of approximately 700 km^2. It is located in the western flank of the Cordillera Central where it reaches its maximum altitudes in the volcanic complex of Nevado del Ruiz-Tolima. The westward margin is formed by the Cauca river. The study area for the medium scale has a size of about 280 km^2 and is located between Manizales and Chinchina.

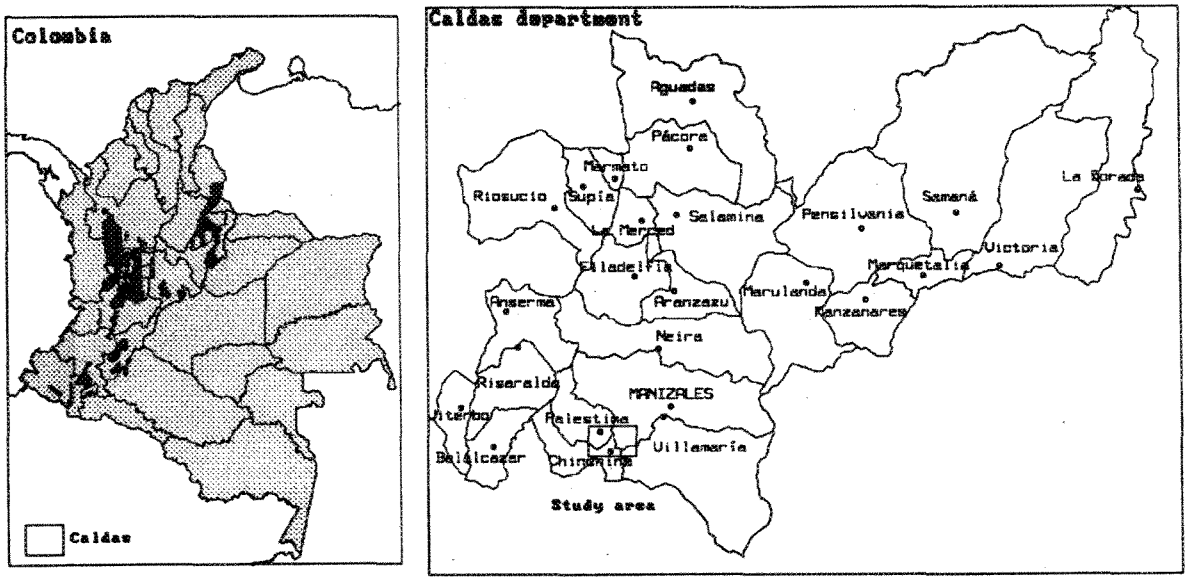

Figure 1: Location of the study area. Left: Overview map of Colombia with areas with major landslide problems displayed in darker grey and the Caldas department with darker boundary. Right: Municipalities within Caldas with the location of the study area.

The data from this paper are from the southwestern part of the medium scale zone, with an area of 68.3 km^2 and inbetween the following coordinates:
Lower left corner: x=827275 y=1041000
Upper right corner: x=837000 y=1048000
The area is located at the western boundary of the Romeral faultzone, consisting of a series of parallel faults with a N-S orientation.

This faultzone has important implications for the lithological distribution, the geomorphology, the landuse and, as we want to know especially, the landslide distribution. The lithological units all have a North-South orientation as well. In the East part the area is underlain by cretaceous metasedimentery, Flysch type rocks, with intercalating subaquatic lavas. At the western margin of the Romeral fault zone, two fault controlled intrusives form the division between rugged topography in the East and smooth topography in the West. West of the Romeral zone the most common rocktype is schist from Cretacious age.
The Romeral faultzone is bordered in the West by a graben structure, which has been filled up by debris flows and pyroclastic flows, pyroclastic fall material and alluvial material. Almost the entire area is covered by a sheet of pyroclastic fall material with a clayey/silty texture. These ashes, which are partly weathered, are very discontinuous in depth, due to differences in pre-ash topography and posterior erosion. From the measured ash profiles no clear relation of ash-thickness with slope angle could be obtained.
As will be shown later, landslide problems are most severe in the Romeral faultzone, especially related to major roads, fault-traces and beginnings of streams. From field observations also a relation was observed between the thickness of the ashes and the occurrences of landslides (see also Van Asch, this volume).
The predominant landuse in the area is coffee. Several farming systems exist, and the trend is to shift from traditional coffee with shadow trees and lower density of plants, to other varieties which do not need shadow trees and have a much higher production.

Input data
The input data for the hazard analysis was obtained partly from existing maps and reports, and partly from newly gathered data by photo-interpretation, field checks, field descriptions and tests, and laboratory tests.
From the overall data set the following maps were used in the analysis presented in this paper:
- Digital Terrain Model
- Slope angles
- Geomorphological main units
- Geomorphological subunits
- Landslide types and activities from different periods
- Geological units
- Faults and lineaments
- Landuse from different periods
- Drainage
- Roads and other infrastructure

All maps were rasterized with a pixelsize of 12.5 meters, resulting in maps of 561*779 pixels.

Geomorphological subunits
Geomorphological maps were made by detailed photo-interpretation and subsequent field checking. For the interpretation the 1:10000 photos were used, together with 1:30.000 photos and a 1:100.000 scale SPOT stereo image for the general overview. Existing geomorphological reports of Florez (1988) IGAC (1988) and Cortez (1988) were used. Two different levels of geomorphological units were outlined: mainunits and subunits. The subunits are the smallest homogenous units that can be mapped on a 1:25.000 scale.

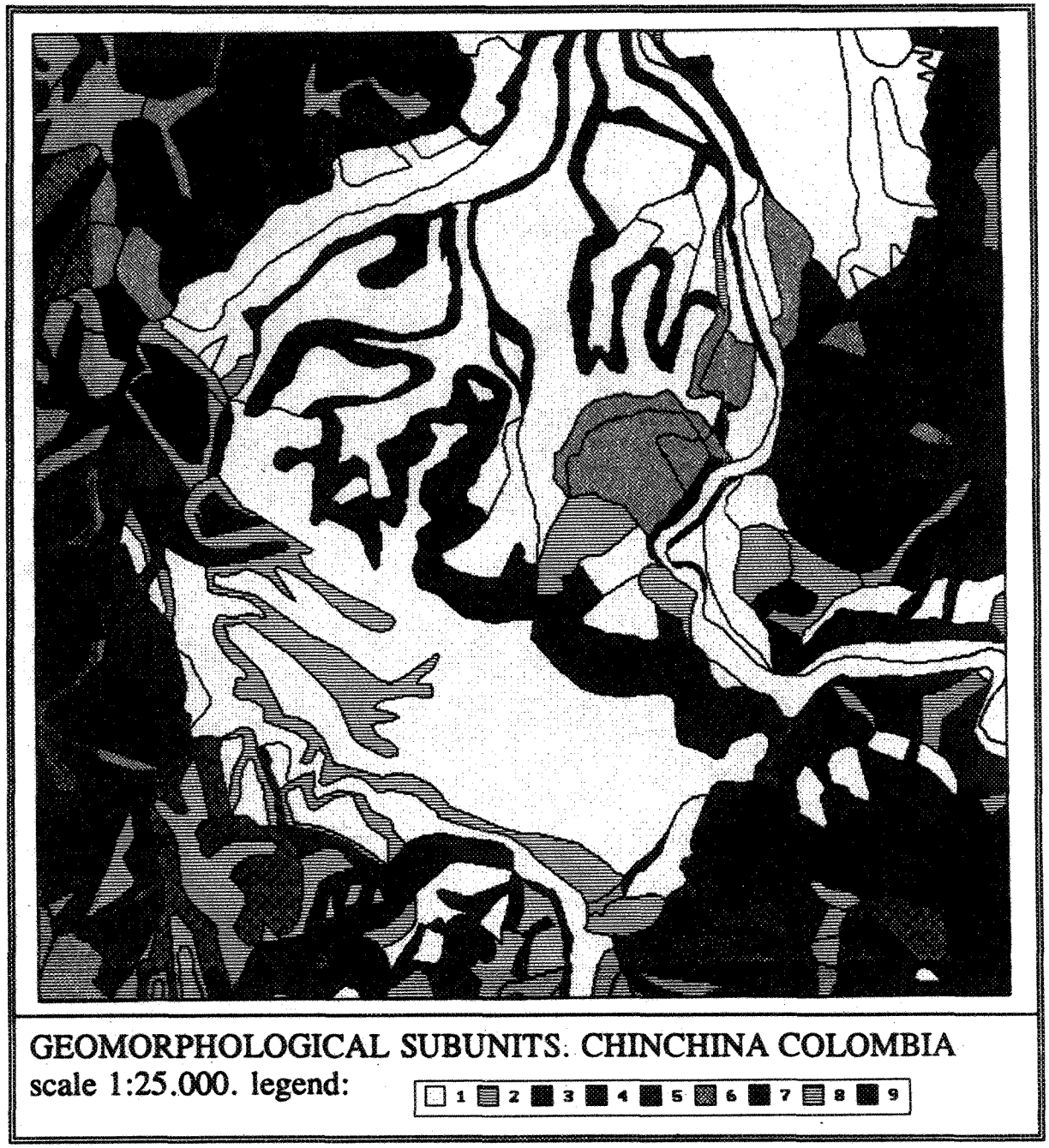

Figure 2: Geomorphological map : subunits (scale 1:25000) The classified map in 9 units, see table 1.

SIMPLIFIED LEGEND FOR GEOMORPHOLOGICAL SUBUNITS	5 Mainly fluvial valleys Division in depth and slope form
1 Alluvial and fluvio-volcanic units Floodplain, terraces and alluvial fans	6 Large mass movements and erosion Division in type
2 Denudational hilltops, ridges and subhorizontal slope sections Division in width and slope form.	7 Denudational structural niches and ridges Division in lithologically or fault related
3 Denudational slopes Division in length and slope form	8 Denudational structural slopes Division in litholgically or fault related
4 Denudational niches Division in length/width ratio and slope form	9 Anthropic landforms. Levelled area, fills, quarries, stabilized slope

Table 1: Simplified legend of geomorphological subunits.

The legend of this map is fairly complex, with about 60 legend units, including genesis and morphography (especially slope length and slope form). However, it can be simplified in nine units when the morphographical factors are not used. The simplified map is given in figure 2 and the simplified legend is given in table 1.

Geomorphological mainunits
In the map of the mainunits, the subunits have been grouped together in one type of terrain, defined by genesis. Both maps can be used as homogenous units for statistical analysis on two levels of detail. To prevent an extreme large number of legend units, it was decided to use this two level approach. It is possible for example that there are denudational subunits present within mainunits of alluvial origin.

Geology
Lithological information was taken from existing geological maps (Naranjo 1989, CHEC 1985, INGEOMINAS 1975, James and Mejia, 1988), SPOT stereo and airphoto-interpretation and additional fieldwork. Rocks were described in the field, using check-lists and taking measurements of joint spacing and the resistance with the Schmidt Hammer. The existing geological maps differed considerably with respect to the displayed faults. Therefore major emphasis was given to the SPOT interpretation. Lineaments not mentioned in any of the reports, and without observed field evidence were not mapped as faults but as photogeolic lineaments. To prevent problems with wrong overlapping of related maps in GIS, caused by digitizing the same boundary two times, the geological map was digitized on the basis of the geomorphological map. Distances were calculated from the faults and lineaments and the distance values were classified in 5 classes (0-50, 50-100, 150-200 and >200 meter from fault)

Slopes
Although parts of the area are covered by 1:10000 and 1:2000 scale topomaps, the only topographical map available for the whole area is the 1:25000 sheet 205-IV-C, with a contour interval of 50 meters. This is unfortunately not very detailed for the production of an accurate Digital Terrain Model. All contours were digitized, rasterized and interpolated, after which filters were used to create slope and aspect maps. The slope map was classified in classes of 10 degrees.

Landuse
Recent landuse information on the parcel level from the national coffee organization was available at a very detailed scale (1:10.000). On these maps (Federacion 1990) the farms and parcels are indicated with unique codes. For each parcel the dominant landuse is given. The digitizing of these maps was an extremely time consuming work. Unfortunately data was lacking for Villa Maria, and therefore it had to be made via photo interpretation.The landuse classification is very detailed, including more then 100 classes, under which the different varieties in farming systems of coffee. The map was classified in only a few classes: bare, grass, shrubs, technified coffee with trees, technified coffee without trees, traditional coffee, other crops, forest and constructions.

Landslide occurrence maps

The landslide occurrence map is crucial in the analysis, since it is based on the presumption that the conditions under which failure took place in the recent past, will be comparable with those that will cause landslides in the near future. Therefore, the accuracy of this map should be high, both in the correct location of the landslide phenomena, as in its correct classification. The landslide occurrence map of the study area is based primarily on detailed photo-interpretation, with additional fieldcheck. For the photointerpretation three series of black&white photos were interpreted:
- 1:10.000 scale from 1981-1987
- 1:25.000 scale from 1965-1969
- 1:30.000 scale from 1947-1949

All three photo-sets were interpreted using a photo-checklist (see table 2).

	TYPE	SUBTYPE	ACTIVITY	DEPTH	VEGETATION	SCARP-BODY
1	Slide	Rotational	Stable	Surficial	Unvegetated	Scarp
2	Flowslide	Translational	Dormant	Deep	Small vegetation	Body
3	Flow	Complex	Active		Large vegetation	
4	Derrumbe					
5	Creep					

Table 2: Checklist used in the photo-interpretation

The original checklist that was used was a much longer one, including factors on dimensions, possible causes, observed damage etc. However, using such an elaborate checklist proved to be impractible for two reasons:

* it was too time-consuming and tiring, to shift every time from the stereoscope to a table for each landslide.
* many of the factors are difficult to determine from airphotos, and would lead to too subjective results.

It was decided not to use complicated landslide classification systems, but to base oneself on the information that could be extracted from aerial photos's for a large number of landslides. The landslide type indicated in table 2 with its Spanish name "derrumbe" stands for debris avalanches; a very fast surficial, mostly translational failure of the soil. In the area most of the "derrumbes" are however not in debris, but in weathered pyroclastics. The degrees of activity that are given in the checklist of table 2 are more degrees of "freshness" of the landslide, as it is often very difficult to separate "activity" from "relative age". For the division of depth into superficial or deep, a qualitative rule of a boundary in the order of 5 meters was used. Most landslides in the area are of the surficial type. Scarps and accumulation zones were identified and mapped separately, as long as the size of the phenomena in relational to the map scale did permit that. Every landslide obtained a unique identifier, in the form of a sequential number, followed by a six digits code, composed of the values from the checklist.

In figure 3 a portion of the landslide map is given for the area surrounding the city of Chinchina.

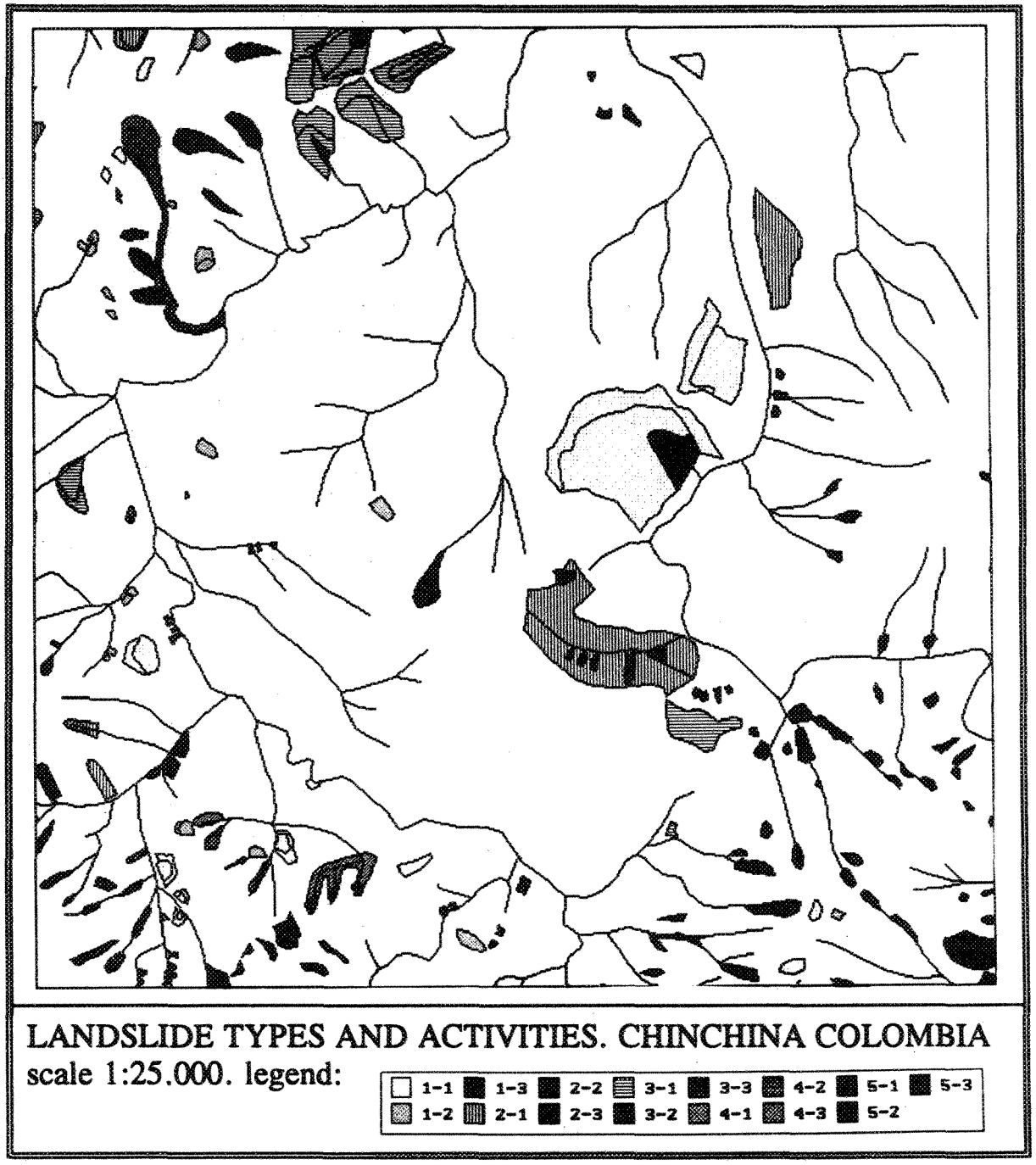

Figure 3: Landslide occurrence map (1:25000 scale) of the area surrounding Chinchina. A combination of landslide type (first number) and activity (second number) is given. Type: 1=Rotational slides, 2=Translational slides, 3=Flowslides, 4=Flows, 5=Debris avalanches "Derrumbes". Activity: 1=Stable, 2=Dormant, 3=Active

Descriptive statistics

After digitizing, checking and polygon coding of the landslide occurrence map, a raster map can be made with an accompanying information table, which gives, apart from the six parameters used in the code, the area and the perimeter of each landslide. Based on this table a number of descriptive landslide statistics could be calculated, such as the total area occupied by landslides, the total number of landslides, the landslide density based on pixels, the number of landslides per square kilometer and the average landslide area. The parameters can be calculated for all slides together, for the different types, for the different activity classes and for the scarps or bodies only. Some examples of these descriptive parameters for the Chinchina dataset are given in table 3 and 4 and in figure 4.

	Bodies	Scarps	Total landslides
number of units	240	802	1111
average area in m^2	6949	2851	4371
Standard deviation in m^2	12115	5315	10710
Minimum area in m^2	234	40	40
Maximum area in m^2	142820	84808	200915

Table 3: Summary statistics for landslide areas

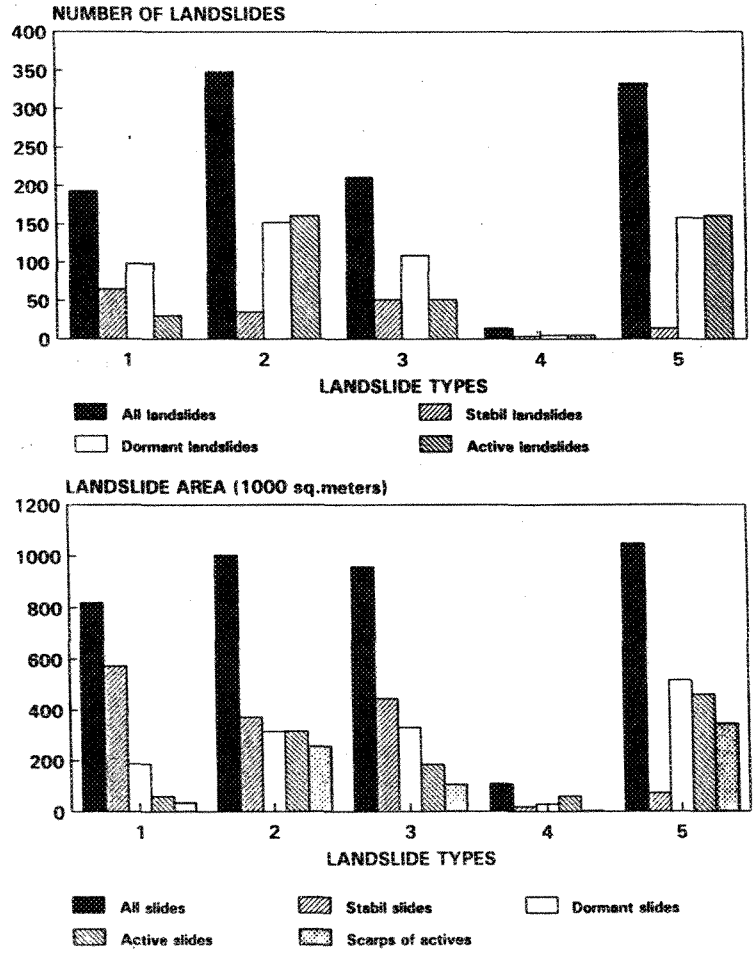

Figure 4. Above: Number of landslides within the sample area. Below: Area of landslides within the sample area. Size of total area 68.3 km^2

Landslide type	AREA M^2	DENSITY promille	NUMBER	NR/KM^2	PERC TOTAL
ALL LANDSLIDES					
- Without distinction	$39.541*10^6$	57.89	1111	16.26	100
- Only active ones	$10.816*10^6$	15.84	408	5.97	36.7
- Only scarps of actives	$7.494*10^6$	10.97	345	5.05	31.1
ROTATIONAL SLIDES					
- Without distinction	$8.333*10^6$	12.20	205	3.00	18.4
- Only active ones	$5.884*10^4$	0.86	30	0.44	2.7
- Only scarps of actives	$3.580*10^4$	0.52	26	0.38	2.3
TRANSLATIONAL SLIDES					
- Without distinction	$1.004*10^6$	14.70	348	5.10	31.3
- Only active ones	$3.169*10^6$	4.64	161	2.36	14.5
- Only scarps of actives	$2.578*10^6$	3.77	147	2.15	13.2
FLOW SLIDES					
- Without distinction	$9.593*10^6$	14.05	211	3.09	19.0
- Only active ones	$1.848*10^6$	2.71	51	0.75	4.60
- Only scarps of actives	$1.053*10^6$	1.54	31	0.45	2.8
FLOWS					
- Without distinction	$1.085*10^6$	1.59	14	0.20	1.3
- Only active ones	$5.984*10^4$	0.88	5	0.07	0.45
- Only scarps of actives	$4.575*10^3$	0.07	2	0.03	0.18
SLIDE AVALANCHES					
- Without distinction	$1.049*10^6$	15.36	333	4.88	30.0
- Only active ones	$4.612*10^6$	6.75	161	2.36	14.5
- Only active scarps	$3.462*10^6$	5.07	139	2.04	12.5

Table 4: Calculated landslide densities for different types and activites within the study area.

Multitemporal photointerpretation

The multitemporal photointerpretation was done by one person, going from the recent set of photos to the oldest ones. In this way it was prevented that inconsistencies occurred between the various maps. However, the process is a very time-consuming one, and one often has to change from one set of photos to another for comparing the different situations. The importance of this multitemporal interpretation is to find those landslides that have appeared newly or that have increased in activity inbetween two periods. There are some factors that are of importance in this respect:

* if landuse changes have taken place inbetween two periods, it may be that new landslides have occurred that were not visible befor, or that, due to less vegetation cover, existing landslides can be better detected.
* the difference in quality and scale of the photos from different periods may cause errors in identyfying long existing landslides on recent, large scale photos, which were not seen on poor quality, old photos, and which are falsely classified as recent slides.

The landslide occurrence maps from the sixties and the forties were made by deleting segments from the eighties map, in that way preventing errors in the location when overlaying the various times. Two landslide occurrence maps were then combined in the GIS in a landslide activity map, which displays all changes in activity between two period

Parameter crossing

In order to evaluate the importance of each of the individual parameter map, crossing between this map and a landslide occurrence map is performed. From the resulting crosstable the landslide densities can be easily calculated.
The following parameter maps were used for the calculation of densities (table 5):

File	Nr Classes	Parameter	File	Nr Classes	Parameter
DTMC	9	Classified heights (100 m.classes)	DR5	3	Distance to 5th order drainage
SLOC	9	Classified slopes (10 degr. classes)	DRT	3	Distance to all drainage
GEOE	52	Geomorphological subunits	DRS	3	Distance to beginning of drainages (25 m. classes)
GEOS	9	Simplified subunits	F1	5	Distance to faults in Romeral system (50 m. classes)
GEOM	27	Geomorphological mainunits	F2	5	Distance to faults W. of Romeral (50m. classes)
CONC	4	Slope convexity	F3	5	Distance to all faults
LUSE	9	Land use (simplified)	F4	5	Distance to all lineaments (50 m. classes)
DR1	3	Distance to 1sr order drainage (25m.)	F5	5	Distance to all faults and lineaments.
DR2	3	Distance to 2nd order	R1	3	Distance to mainroad Manizales Chinchina (25 m. classes)
DR3	3	Distance to 3rd order	R2	3	Distance to all mainroads (25m. classes)
DR4	3	Distance to 4th order	R3	3	Distance to all main and secondary roads (25 m. classes)

Table 5: Summary of the parameter maps with the number of classes and the code of the file

Resulting in a total number of parameter classes of 174.
The density was calculated for:
a. total number of landslides (undifferentiated)
b. each landslide type separately (5)
c. each active process per type separately
d. each active scarp per type separately.
Without any problem the calculations could also be done for stabil or dormant ones, but that was not considered neccessary. Batch files were written where the whole process of map crossing and density calculation was performed automatically from an input table with the names of the files. Also graph plotting for the evaluation of the results was built-in. This resulted in a number of 12 graphs for each parameter. An example of this for slope classes is given in figure 5. As can be seen from this figure the curves for b, c and d more or less follow the same trend. From this one can conclude that, at least for this area, there will not be so much difference in the result if all the slide of a single type are used, and not just the active ones, or the actice scarps. The only clear difference is for rotational slides, where from the comparison of the three curves for percentage area can be seen that the stabil slides appear in lower slope ranges.

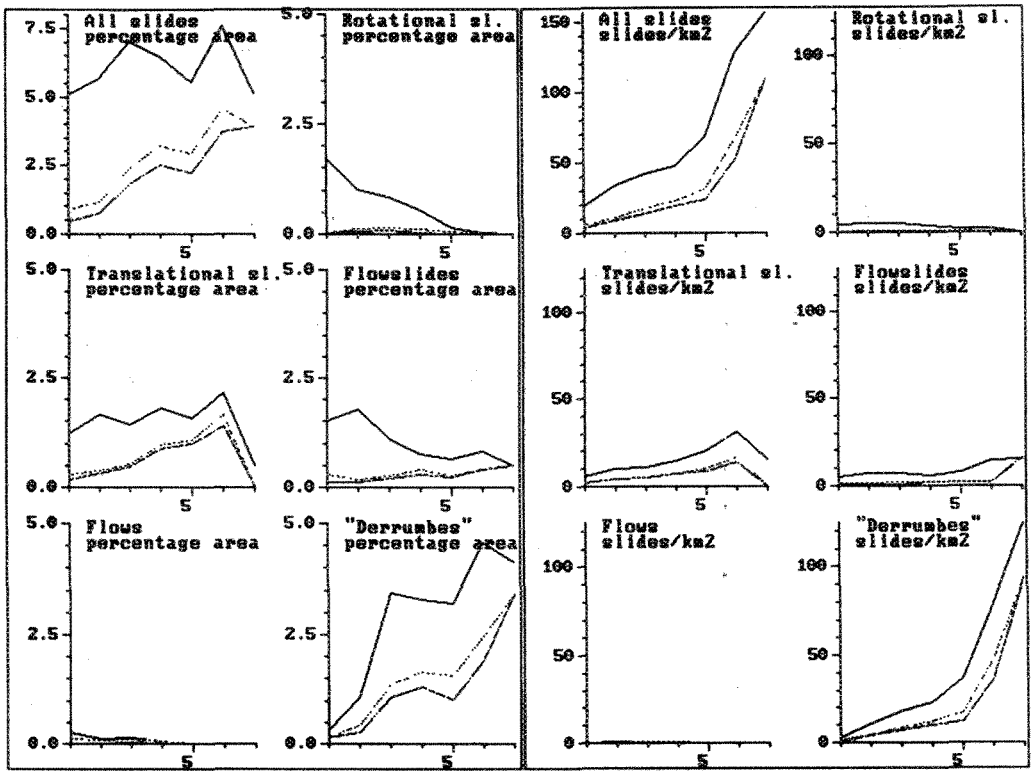

Figure 5: Example of results for the density calculation of slope classes. The figure displays two blocks of 6 graphs. The left block is for density expressed in percentage of parameter class covered by pixels with landslide. The right block expresses density as number of slides/square kilometer. In each graph there are three lines: the upper represent all stabil, dormant and actives together, the middle line represent all active slides and the lower line represent all active scarps.

For each parameter class and landslide type two types of densities were calculated:
1. Area density = densities expressed as number of pixels with landslides divided by total number of pixels within the parameter class. Depending on the magnitude this was displayed as percentages or promilles.
2. Number density= densities expressed as number of landslide occurrences per square kilometer of area of the parameter class.
The calculation process for density type 1 is a lot simpler with the GIS as it can work with bit maps of landslide occurences (yes or no landslide). For density type 2 one needs to cross the parameter map with a landslide map where each landslide has a unique number, and then later on do table joining in order to find out the type and activity of the landslides.
Comparing the two blocks for the densities based on area and on the number of slides in figure 5, it is clear that there are large differences. The importance of the few, but very large, stabil rotational failures can be observed very clearly. The high densities in the steeper slope ranges are explained by many "derrumbes", which are mostly relatively small in size, and by the fact that these slope ranges are much smaller, so when there are some landslides, the density will go up rapidly.
As can be seen from figure 5 the total number of calculated densities per parameter were 2(density types)*6(landslidetypes)*3 (activity type)= 36 * 174 (total number of parameter classes)=

6264 different density values to evaluate on their importance for landsliding. To facilitate this process a weighting factor was introduced which was defined as follows:

Weight= (calculated density)-(overall density)

The overall densities are the values displayed in table 4.
To give an example: If within a parameter class there is a density of active translational slides of 35/km^2, and the overall density of active translational slides in the whole area is 2.36/km^2, the weighting value will be 32.64. In this way both positive and negative weights can be applied to the parameters, and the importance of different parameters can be compared.
In table 6 and figure 6 the weight values for the two density types calculated for the undifferentiated group of all landslides are compared. The values displayed in figure 6 are a random selection of a third of all 174 parameter classes. What is clear from this table is that the weight values based on area of slides are not so variable as those based on number of slides/km^2.

	Min	Max	Avg	Nr <-5	Nr -5-0	Nr 0-5	Nr 5-25	Nr 25-50	Nr >50
Area	-5.7	94	0.748	16	91	62	12	0	2
Number	-16.3	177	12.93	30	23	32	58	33	7

Table 6: Comparison of weight values for all the parameter classes for the density based on area, and the one based on number of landslides

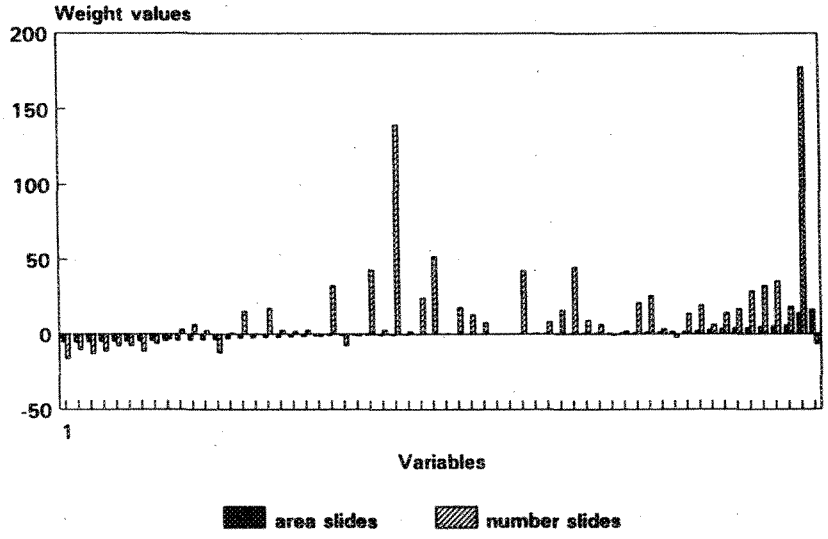

Figure 6: Comparison between weight values based on area and on number for a third of the 174 parameter classes.

In table 7 the weight values are ranked according to the density in nr/km^2. It can be seen from this table that the geomorphological units related to the terraces receive negative weights as well as the units from the geological map related to these terraces. The highest scoring variable is the distance of less than 25 meter from the beginning point of streams, where water concentration takes place, and where there are 177 slides/km^2 more than one would expect.

Density nr/km²	Density pixel%	Class	Variable
-16.300000	-5.789300	8	slopeclas
-16.300000	-5.789300	10	geom-mainunit
-16.300000	-5.789300	45	geom-subunit
-16.300000	-5.789300	47	geom-subunit
-13.469140	-5.349928	3	geom-subunit
-12.538060	-3.555648	4	geom-mainunit
-12.039010	-5.345447	4	geom-subunit
-12.019470	-5.015365	9	geology
-11.557500	-4.825980	7	geom-subunit
-11.397420	-5.254473	4	concavity
-11.264590	-5.710622	5	geom-subunit
-11.186410	-4.912787	1	geomsimple
-10.809030	-4.476615	9	geom-subunit
-10.656260	-5.701117	8	geom-subunit
-10.401160	-4.860233	5	geom-mainunit
-10.023690	-4.461306	12	geom-mainunit
-9.914597	-5.532744	1	fift-order
-9.619415	-4.838245	1	geom-mainunits
-9.490040	-5.094117	1	geom-subunit
-9.226280	-0.802195	11	geology
-8.232332	-3.979346	21	geom-subunit
-7.936010	-4.903530	6	geology
-7.908391	-5.089999	13	geom-subunit
-7.823181	-1.021090	12	geom-subunit
-7.104597	-5.501944	11	geom-subunit
-6.695938	16.281580	17	geom-mainunits
-6.392266	-4.612757	9	geom-mainunits
-5.842480	-3.828516	49	geom-subunit
-5.549210	-1.141139	2	dtmclas
-5.027430	-2.795024	27	geom-mainunits
-4.997569	-3.096143	25	geom-subunit
-4.385849	-2.011377	6	geom-subunit
-4.247270	-4.157160	3	geom-mainunits
-3.806970	-4.613282	2	geom-subunit
-3.344529	-4.473511	26	geom-mainunits
-3.265940	-0.134562	2	geology
-2.312089	1.548111	7	geology
-1.558680	-1.288946	18	geom-subunit
-1.544959	-4.578925	8	geology
-1.228339	-0.905829	3	first-order
-0.825489	0.698711	2	geom-mainunits
-0.578059	0.583528	5	geology
-0.378940	-0.769247	3	geology
-0.347690	-1.432757	7	dtmclas
-0.266920	-0.551610	3	all_drainage
-0.259899	-4.118457	18	geom-mainunits
-0.229460	-0.101570	2	mainr-man-chin
-0.192539	-2.632142	2	geomsimple
-0.192099	-0.014882	5	romeral-faul
-0.175508	-2.639986	43	geom-subunit
-0.101700	-0.180676	2	mainroads
-0.056348	-3.758843	50	geom-subunit
-0.039239	-0.618287	3	begin-1-order
BLOCK OMITTED BETWEEN 0 AND +10			
10.026390	1.048342	23	geom-mainunits
10.041190	3.098722	2	concavity
10.139730	3.654639	12	geology
10.175630	-0.120851	6	landuse
11.059330	0.570117	7	landuse
11.563690	-3.987768	1	fourth-order
13.036550	-0.119819	28	geom-subunit
13.057800	-5.330584	48	geom-subunit
13.303420	0.906350	2	landuse
13.421350	5.422550	23	geom-subunit
13.606530	1.593875	25	geom-mainunits

Density nr/km²	Density pixel%	Class	Variable
13.940030	1.235207	27	geom-subunit
14.198220	3.395714	33	geom-subunit
15.320550	-2.726059	31	geom-subunit
15.875500	0.335014	15	geom-subunit
16.053870	-0.891986	19	geom-subunit
16.663550	-0.031243	10	geology
16.894550	1.452973	1	geology
16.963920	3.864367	4	geomsimple
17.137820	-2.288778	44	geom-subunit
17.562430	94.210700	34	geom-subunits
17.596210	-0.131988	2	slopeclas
18.388350	5.694440	22	geom-subunit
19.198170	1.896686	1	all-faults
19.260680	-0.911253	1	third-order
19.695500	-0.277489	8	landuse
19.824280	0.971846	1	faults&lines
19.944830	0.200680	1	west-faults
19.953770	1.584188	40	geom-subunit
20.694220	-0.779666	16	geom-mainunits
20.899830	0.960805	39	geom-subunit
22.675880	3.991956	29	geom-subunits
23.335360	2.248844	1	all_drainage
24.096920	-1.371946	2	all_drainage
24.136680	-0.370817	1	lineaments
24.617640	1.619500	30	geom-subunits
25.066880	-1.107014	2	first-order
25.570350	1.215658	3	slopeclas
26.188810	-2.284591	2	fourth-order
26.233760	4.854520	7	geom-mainunits
26.568880	-0.702412	1	romeral-faul
27.253000	14.670940	26	geom-subunit
28.907270	4.118968	5	geomsimple
29.471140	1.583557	1	main&sec-roads
29.563710	-0.726859	1	second-order
30.164940	0.733488	2	all-faults
30.998380	0.672252	4	slopeclas
32.237380	0.819584	9	dtmclas
32.333340	4.850690	1	first-order
32.337890	-1.124272	4	west-faults
32.728400	5.215930	6	geom-mainunits
33.085360	0.435568	2	faults&lines
34.114430	0.371419	4	all-faults
35.385090	5.255140	32	geom-subunit
36.049750	0.366049	4	faults&lines
36.922470	0.227578	2	west-faults
37.522640	-0.931084	2	third-order
41.538540	-0.123446	4	lineaments
42.136810	4.510190	3	landuse
42.254980	0.068085	2	lineaments
43.145420	-0.789984	3	west-faults
43.821060	-0.109715	2	second-order
43.879040	0.088186	3	fault&lines
44.568230	0.377290	3	all-faults
45.422150	-0.048771	2	romeral-faul
45.611160	5.457330	1	mainroads
45.916230	-0.365029	3	lineamenents
47.657710	-0.140142	3	romeral-faul
48.664620	0.554901	4	romeral-faul
51.899940	-0.238855	5	slopeclas
54.474090	16.485580	38	geom-subunit
66.724290	3.866443	2	begin-1-order
91.295300	9.641500	1	mainr.-man-chin
111.36280	1.775623	6	slopeclas
139.41780	-0.679811	7	slopeclas
177.59770	13.720800	1	begin-1-order

Table 6: List of negative and extreme positive weight values. The group with weight values from 0-10 has been omitted.

Among the high scoring parameters is also a distance of less than 25 meters from the mainroads with an extremely high value for the mainroad from Manizales to Chinchina (see also figure 7).
This figure serves also to demonstrate the importance of selecting the right parameters. The main and secondary roads altogether, which also run through flat or hilly terrain, has a much lower weighting value than the mainroad from Manizales to Chinchina which crosses the Romeral zone in E-W direction.

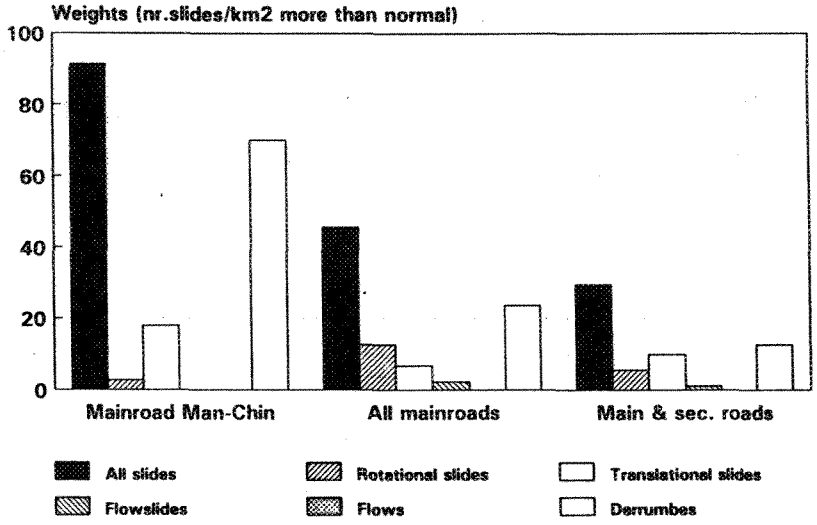

Figure 7: Weight values for three different subsets of roads.

Susceptibility maps
With a number of input maps of 22 (table 5) and 36 different ways to use each them with weight values (figure 5), the amount of different susceptibility maps that one could make are impressive. Therefore one should select a small set of maps with the highest relevance.
Based on the results given in table 7 various input maps were combined, by simply adding up the weight values.
A batch file was made where the user can enter the output map, the type of process for which the map should be made and the variables that should be used to combine them. The input maps are then renumbered with the weights and the maps are summed. After that the result map can be classified into three, or more classes, using an automatic classification, based on histogram calculation, or by decision rules that were given by the user.
Figure 8 gives an example of a susceptibility map for debris avalanches (derrumbes) based on the combination of slope, geology, geomorphological subunits, landuse, faults, mainroads and beginning of first order streams. The map is classified in four groups. Group 1 are all those areas that result with negative, or zero weighting values. These are basically the terrace areas around Chinchina and the floodplains.
The exactness of the output map can be checked by crossing it with the original landslide map and evaluate how many landslides occur in zones which come out as safe on the map.
As can be seen clearly from the map in figure 8, the dots represent those areas near the beginning of streams. Because of their very high weighting factor (177) they show up in all

places, even on the terraces. Although they do represent also there a slightly higher possibility for failure, they should not be represented as high hazard. The same is true for the faults, which give also weighting values, when they cross a floodplain. To prevent these errors, more attention should be given to the selection of the input variables. It is better to seperate files with the same type of information (roads, faults, drainage etc) in different sets related to the different major terrain divisions.

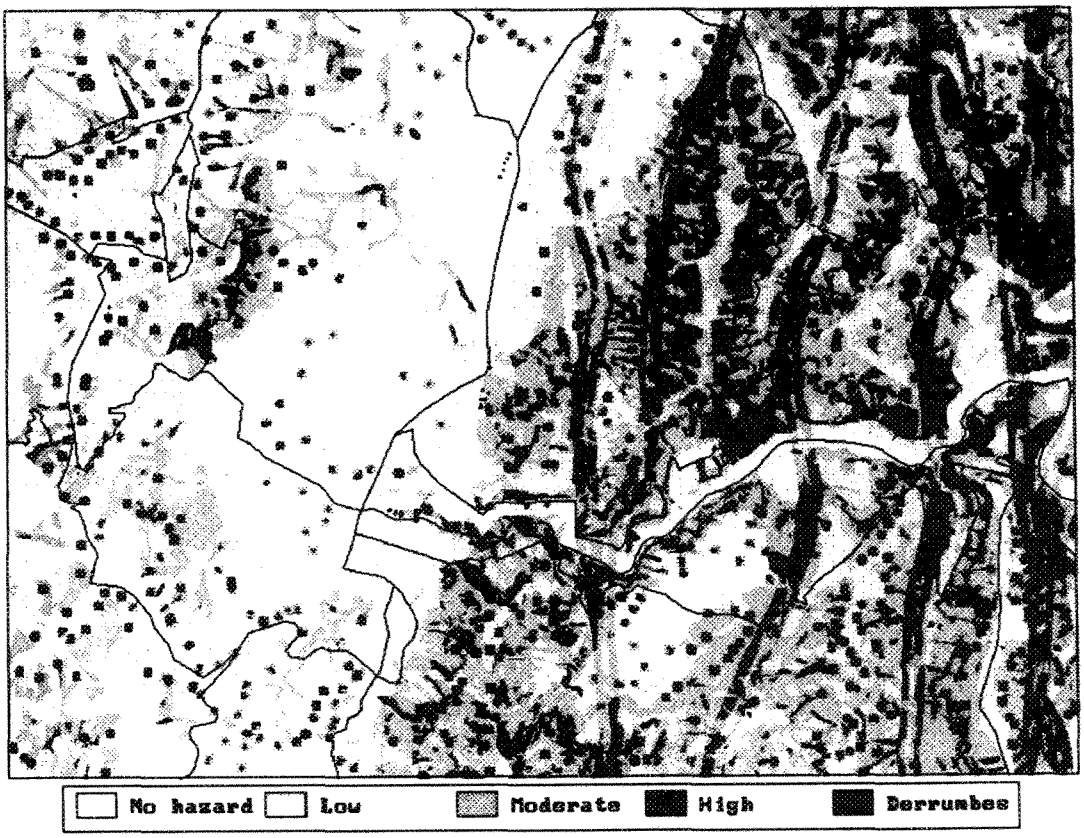

Figure 7: Example of a susceptibility map, made by combining geology, geomorphology, landuse, slopeangle and beginning of first order streams

Conclusions

From the comparison of the weight values based on area and on number of landslides it can be concluded that the latter gives a better variation in values.

For the creation of susceptibility maps there is not such a large difference if one doesn't distinguish in activity class, however we do advise to do that, in order to evaluate the importance of active slides as compared to dormant and stabil.

The selection of parameters is the most crucial part in the analysis. By splitting up parameters in more classes, much higher weights can be obtained.

The method proved to be useful in the evaluation of parameters and the creation of a quantitative hazard map.

References

CHEC (1985)
Evaluacion de los recursos geotermicos del area San-Vicente-Manizales-Tolima. G
Geologia Regional, Manizales, Colombia, 110 p and map

Cortez, R. (1988)
Estudio de deslizamientos en el triangulo vial Manizales.
Proyecto MPOT-UN, Bogota, 79 p.

Federacion Nacional de Cafeteros (1990)
Manual para el dirigamiento del formulario para el inventario de las fincas en la zona cafetera de los municipios Manizales, Chinchina y Palestina.
Landuse maps municipalities Manizales, Chinchina and Palestina, scale 1:10000. Unpub. Manizales, Colombia

Florez, A. (1988)
Geomorfologia del area Manizales-Chinchina. Cordillera Central, Colombia.
Analisis Geograficos No 9, IGAC, Bogota, Colombia, 158 pp.

IGAC (1988)
Estudio geomorfologico, erosion, suelos y uso de la tierra en los municipios de Chinchina, Villamaria, Palestina, Neira, Filadelfia, Pacora y Aguadas, Caldas. Internal report for CRAMSA, Manizales.

INGEOMINAS (1975)
Geologia del quadrangulo K-8
Unpublished 1:100000 scale geological map. INGEOMINAS, Medellin, Colombia

James, M. and Mejia (1988)
Evaluacion amenazas geologicas del area Manizales-Valparaiso.
Interconexion Electrica S.A. Medellin, Colombia, 143p.

Naranjo, J.L. (1989)
Geologia de Manizales y sus alrededores y su influencia en los riesgos geologicos.
Revista Universidad de Caldas, Vol.10 Nos 1-3, Manizales, Colombia, 113 pp.

Soeters, R., Rengers, N. and Van Westen, C.J. (1991)
Remote sensing and Geographical Information Systems as applied to mountain hazard analysis and environmental monitoring
8th Thematic Conf. on Geologic Remote Sensing, Denver, USA, April 29-May 2, 1991, pp 1389-1402

Rengers, N. Soeters, R. and Van Westen, C.J. (1991)
Remote sensing Capabilities for use in GIS, Applied to mountain hazard mapping: Possibilities for today and wishes for development in the future.
ERIM symp. on Remote Sensing in Global Geoscience Processes. Un. Boulder, USA, May 4, 1991.

Rengers, N. and Soeters, R. (1992)
Applicability of remote sensing in GIS for slope instability hazard zonation: a review with emphasis on the aspects of scale and resolution
1st Int. Symp. on Remote Sensing and GIS for natural risk studies. Bogota, 8-15 March, 1992, 6pp.

Rengers, N. (1992)
Mountain hazard mapping in the Andean Environment using Geographical Information Systems; an international research cooperation project.
1st Int. Symp. on Remote Sensing and GIS for natural risk studies. Bogota, 8-15 March, 1992, 6pp.

Valenzuela, C.R. (1990)
ILWIS overview
ITC-Journal 1990-1, pp 4-14

Van Asch, T.W.J. (1992)
The role of water in landslide hazard analysis
1st Int. Symp. on Remote Sensing and GIS for natural risk studies. Bogota, 8-15 March, 1992, 13 pp.

Van Asch, T.W.J., Van Westen, C.J., Blijenberg, H. and Terlien, M.I.J. (1992)
Quantitative landslide hazard analysis in volcanic ashes of the Chinchina area, Colombia

Van Westen, C.J.(1989)
ITC-UNESCO project on GIS for mountain hazard analysis
1st Southamerican Symposium on Landslides, Paipa, Colombia, 7-10 august 1989, pp 214-224

Van Westen, C.J. and Alzate, J.B. (1990)
Analisis de amenazas en areas montanosas, utilzando SIG, basado en un computador personal.
1st Colombian Conference on Environmental Geology, Medellin, Colombia, April 30-May 2, 1990
AGID report no 13, pp 527-536.

Van Westen, C.J. and Alzate, J.B. (1990)
Mountain hazards using a PC-based GIS
6th Int. IAEG congr. proc., Balkema, Rotterdam, pp 265-271

Van Westen, C.J. (1992)
Scale related GIS techniques in the analysis of landslide hazard.
1st Int. Symp. on Remote Sensing and GIS for natural risk studies. Bogota, 8-15 March, 1992, 6pp..